STATIC AEROELASTIC ANALYSIS AND TAILORING OF MISSILE CONTROL FINS

S. C. McIntosh, Jr.
McIntosh Structural Dynamics, Inc.
Mountain View, California

M. F. E. Dillenius
Nielsen Engineering & Research, Inc.
Mountain View, California

PROBLEM DEFINITION

This paper describes a new concept for enhancing the design of control fins for supersonic tactical missiles. The concept makes use of aeroelastic tailoring to create fin designs (for given planforms) that limit the variations in hinge moments that can occur during maneuvers involving high load factors and high angles of attack. It combines supersonic nonlinear aerodynamic load calculations with finite-element structural modeling, static and dynamic structural analysis, and optimization.

The problem definition is illustrated in figure 1. The fin is at least partly made up of a composite material. The layup is fixed, and the orientations of the material principal axes are allowed to vary; these are the design variables. The objective is the magnitude of the difference between the chordwise location of the center of pressure and its desired location, calculated for a given flight condition. Three types of constraints can be imposed -- upper bounds on static displacements for a given set of load conditions, lower bounds on specified natural frequencies, and upper bounds on the critical flutter damping parameter at a given set of flight speeds and altitudes. The idea is to seek designs that reduce variations in hinge moments that would otherwise occur. The block diagram at the left in figure 1 describes the operation of the computer program that accomplishes these tasks. There is an option for a single analysis in addition to the optimization. Additional details concerning this work may be found in reference 1.

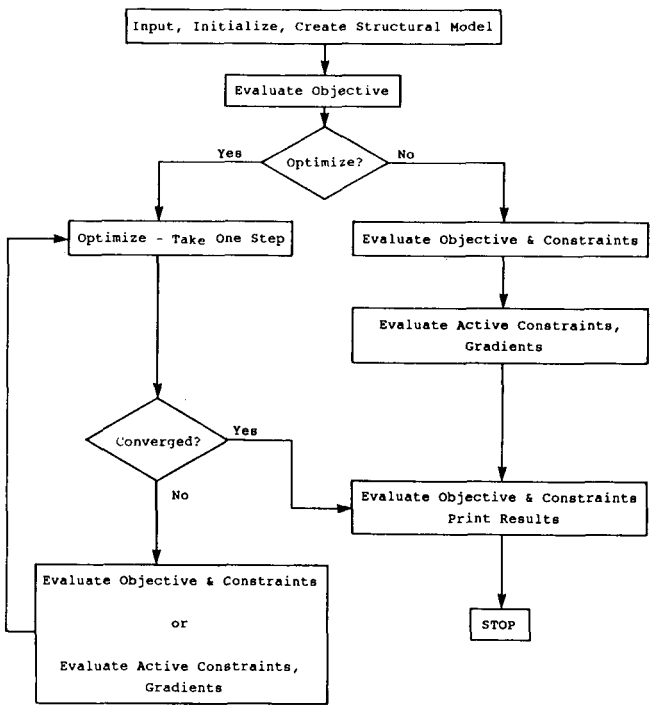

- Objective: Dimensionless chordwise center of pressure offset from desired position, $|x_{cp}/\bar{x}_{cp} - 1.0|$, for a given flight condition.
- Design Variables: Material principal axis directions, θ_i, for a given stacking sequence.
- Constraints: Displacements, $z/\bar{z}_r - 1.0 \leq 0$, for a given set of load conditions

  Frequencies, $1.0 - \omega_r/\bar{\omega}_r \leq 0$

  Flutter Speeds, $g_r - g_r \leq 0$, at fixed speed and altitude.

Figure 1

STRUCTURAL MODEL

The example fin is illustrated in figure 2. It is made up of a graphite/epoxy composite with the stacking sequence as given in the figure. The fin is modeled with triangular bending elements. These are the elements described in reference 2, with modifications for anisotropic materials as given in reference 3. For each element, the orientation of the material principal axes with respect to the element local coordinate axes can be specified. For a given region of the fin, these angles can be specified so that a single angle variable governs the overall orientation. Two such regions, governed by design variables θ_1 and θ_2, are shown in the figure. The outer portion of the fin is inactive for tailoring purposes. The fin is anchored to a fixed node at the hinge line just inboard of the root by a beam-rod whose stiffness properties model the stiffness of the fin actuator and the body backup structure.

To update the design, the fin stiffness matrix for the active regions must be recreated. This is a relatively simple task, since the updating affects only the rotation matrices that transform the element constitutive matrices from principal axes to local coordinate axes. Gradients of the stiffness matrices are obtained analytically by differentiating the expressions for these matrices with respect to the orientation angles. Calculations for the constraints and their gradients follow well-known procedures and will not be discussed here. Reference 1 can be consulted for additional information.

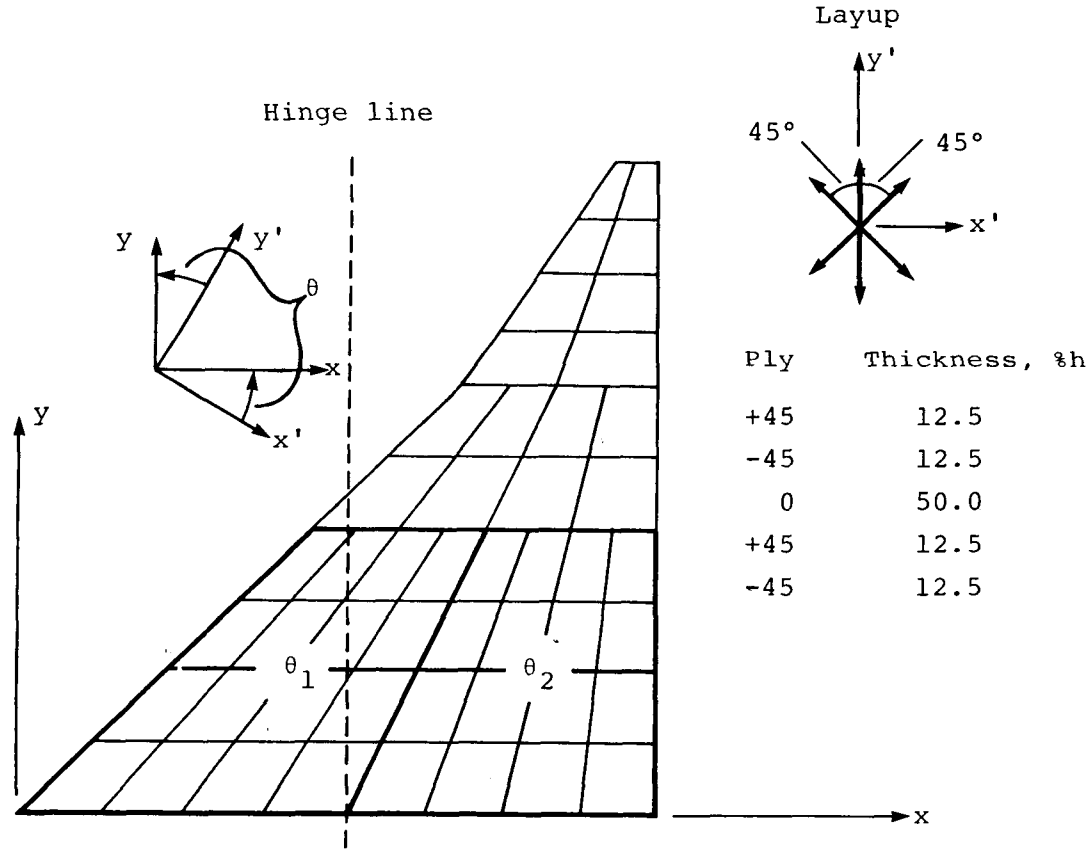

Figure 2

AERODYNAMIC LOAD CALCULATION

The aerodynamic load prediction method (ref. 4) applies to a fin attached to an axisymmetric body. The missile components are represented by distributions of singularities derived from supersonic linear theory. The missile body is modeled with linearly varying supersonic line sources and line doublets. In a finned section, the lifting surfaces and the body portion spanned by the lifting surfaces are modeled with planar supersonic lifting panels. Fin thickness effects can be represented, if desired, by planar source panels. The panel strengths are obtained by satisfying the flow tangency conditions at a set of control points, one for each panel. In addition, the fin loads include nonlinear augmentations due to fin leading and side edge flow separation at high angles of attack, and (for canard fins) nonlinear loads resulting from vortices formed on the forebody for the proper combination of forebody length and angle of attack. The tangency boundary condition satisfied on the fin includes the changes in streamwise slope caused by elastic fin deformation.

To compute the fin deformation, the aerodynamic loads at the control points are interpolated to loads at the structural node points in a scheme that preserves overall fin load and moments. Since the fin loads are in general nonlinear functions of fin deflection, an iterative process, described in detail in reference 1, is used to produce consistent fin deformations and loads. The resultant chordwise center of pressure location is then used to calculate the objective. Gradients of the objective are computed by finite differencing.

The static aerodynamic description of the example fin is given in figure 3. The following flight condition was assumed: An included angle of attack of 15.4 deg, a roll angle of 0.0 deg, a Mach number of 1.6, and an altitude of 30,000 ft. The fin is undeflected. A vertical plane of symmetry is assumed, and the body has an ogive nose up to the fin leading edge. No thickness or nonlinear effects are included in this model.

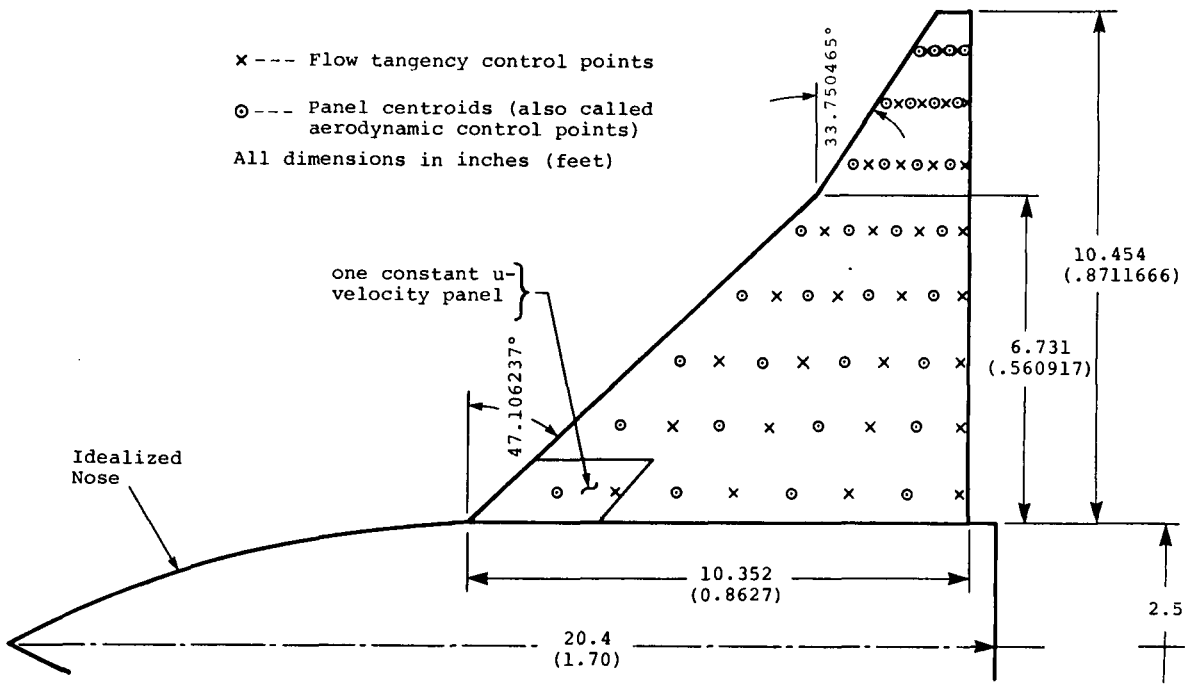

Figure 3

FLUTTER CONSTRAINT

A flutter constraint was the only one considered in this example. The results of a flutter analysis at a Mach number of 1.4 are shown in figure 4, which presents a velocity-damping plot at a match-point altitude of 43,500 ft. Structural damping of 3% is assumed, so the match-point flutter speed is given by the g = 0.03 crossover of the first-mode branch. The flutter constraint requires that the damping parameter g for this branch be less than 0.03 at this speed and altitude.

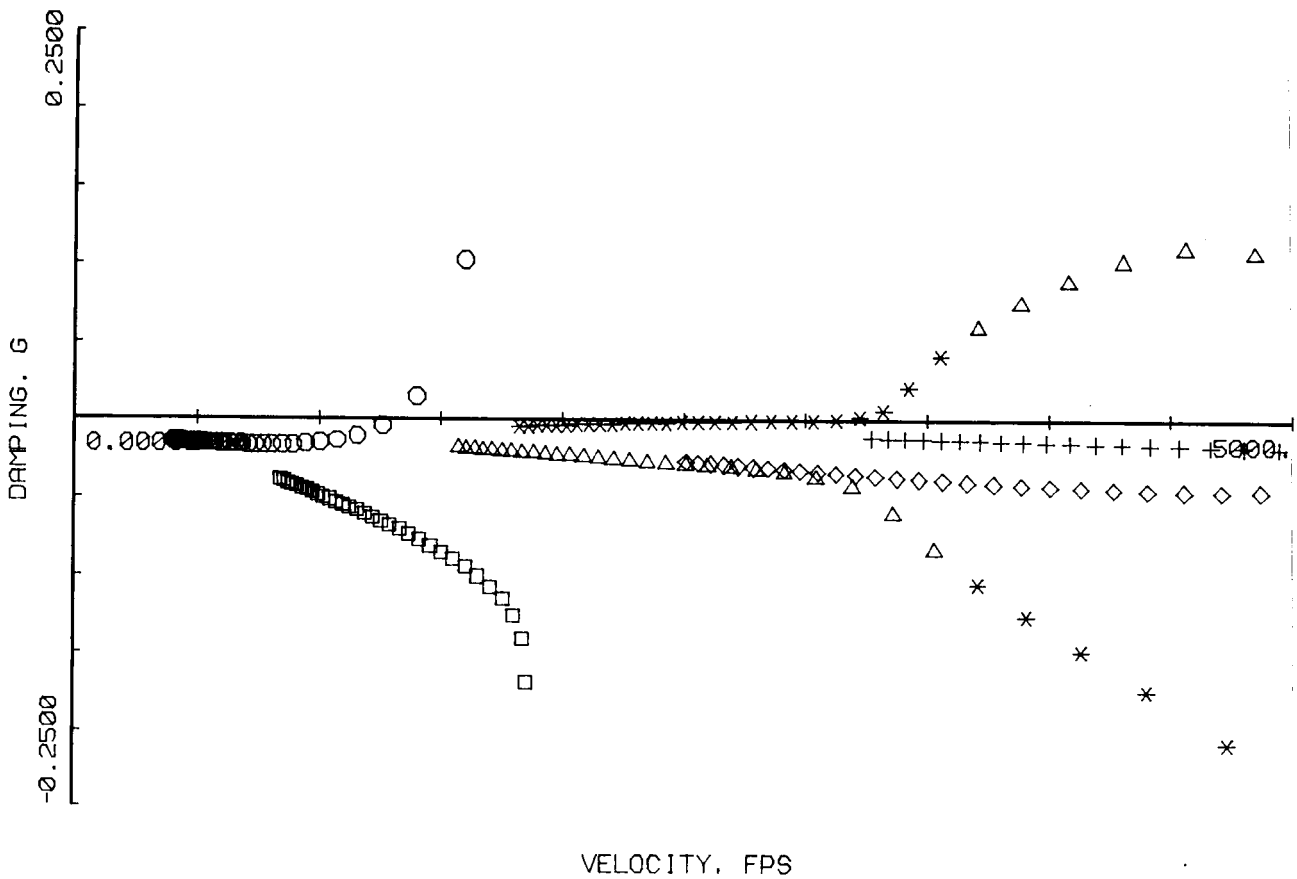

Figure 4

PARAMETRIC SURVEY

To provide some indication of the behavior of the fin as the principal-axis orientations are varied, the analysis-only option of the computer program was exercised. The angles θ_1 and θ_2 were linked to form a single design variable. Figure 5 displays the variation of x_{cp}. In view of the nature of the rotation matrix that transforms each element constitutive matrix from principal-axis to local coordinate directions (see Eq. (4) of ref. 1), the quasiharmonic nature of this variation is not surprising. The location of x_{cp} for the same fin made of aluminum is also shown.

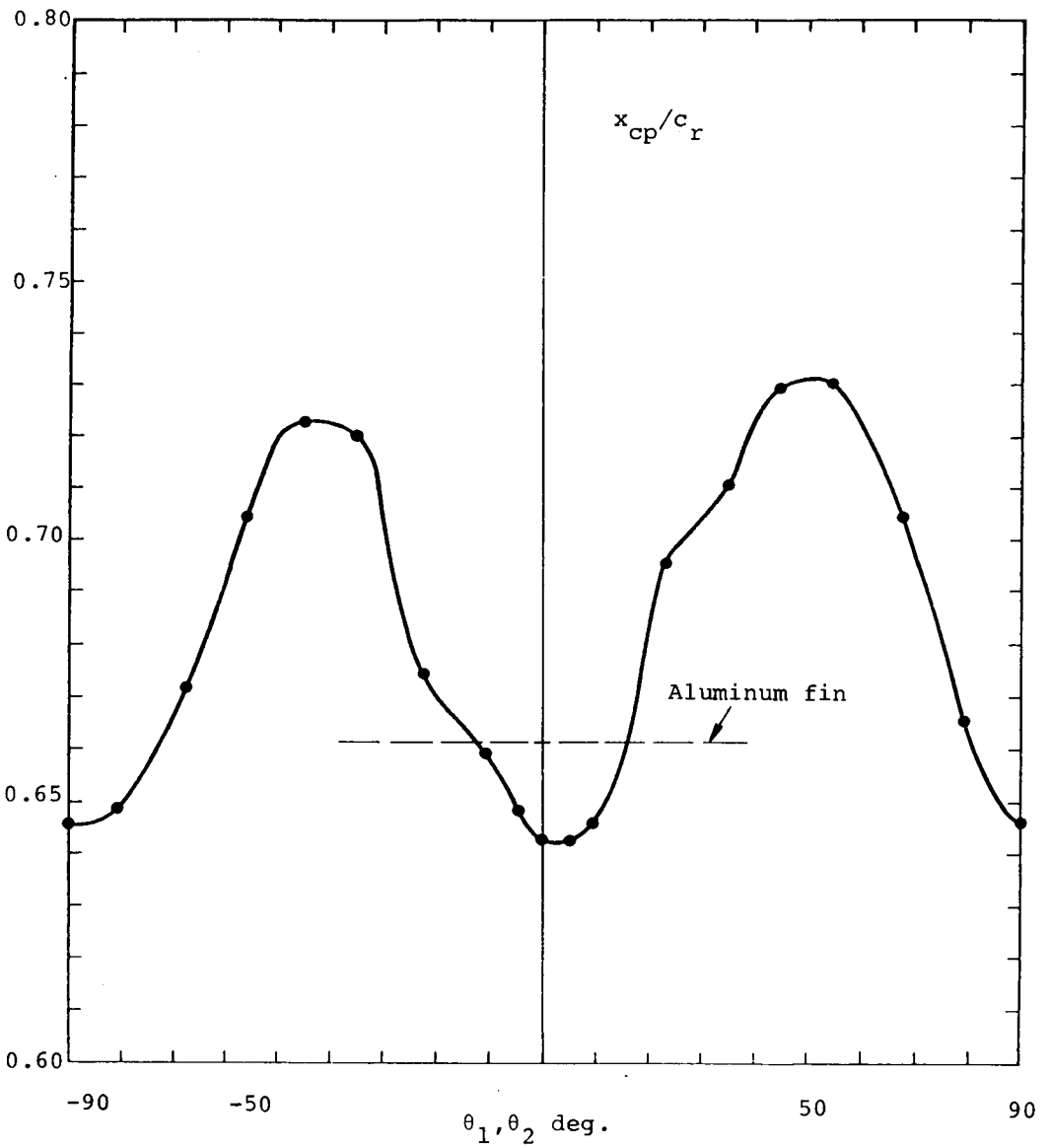

Figure 5 .

FIN DEFORMATIONS

Figure 6 presents perspective plots of the deformed fins for selected values of θ. The view in these figures is outboard in the x-y plane defined in figure 2, so the undeformed fin would be seen as a straight line. With θ near +45 deg or -45 deg, the chordwise flexibility is near maximum, which corresponds to the maximum shift in x_{cp}. Contrary to what might be expected, however, the fin chordwise bending is concave, rather than convex. This reduces the fin loading near the leading edge, so the center of pressure moves aft. Since the center of pressure is always aft of the hinge line, the fin also has a nose-down rigid-body rotation, which also appears in the plots.

When θ_1 and θ_2 are allowed to be independent, the curve in figure 5 becomes the intersection of the $\theta_1 = \theta_2$ plane with the x_{cp} surface. This surface was not mapped extensively, but enough analyses were performed to suggest that the surface resembles the shape of an egg carton, where the minima of figure 5 are the bottoms of valleys, and the maxima are the tops of peaks.

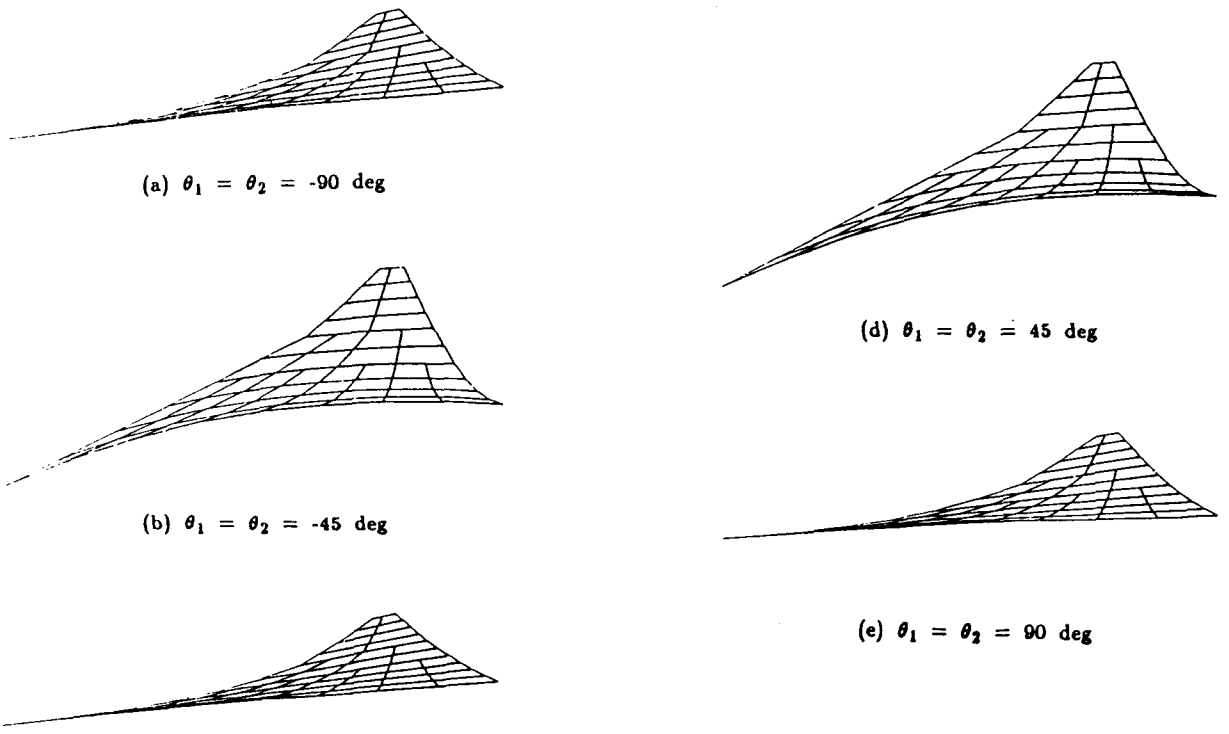

(a) $\theta_1 = \theta_2 = -90$ deg

(b) $\theta_1 = \theta_2 = -45$ deg

(c) $\theta_1 = \theta_2 = 0$ deg

(d) $\theta_1 = \theta_2 = 45$ deg

(e) $\theta_1 = \theta_2 = 90$ deg

Figure 6

OPTIMIZATION EXAMPLE 1

In the first optimization example, θ_1 and θ_2 were linked to form a single design variable. The desired value of x_{cp}, measured from the fin leading edge at the root, was set to 60% of the root chord c_r. The initial value of θ was 0.7 rad, or 40.1 deg. The flutter constraint, fixing the critical-mode crossover at a Mach number of 1.4 and an altitude of 43,500 ft, was also imposed. The iteration history for this example is shown in figure 7. In five iterations, the minimum at θ = 3.43 deg was found. This corresponds very well with the curve of x_{cp} versus θ in figure 6. Attempts to reach the minimum near θ = 90 deg were not successful because the flutter constraint was violated.

The optimization subroutine CONMIN (ref. 5) was used in all of the optimization examples.

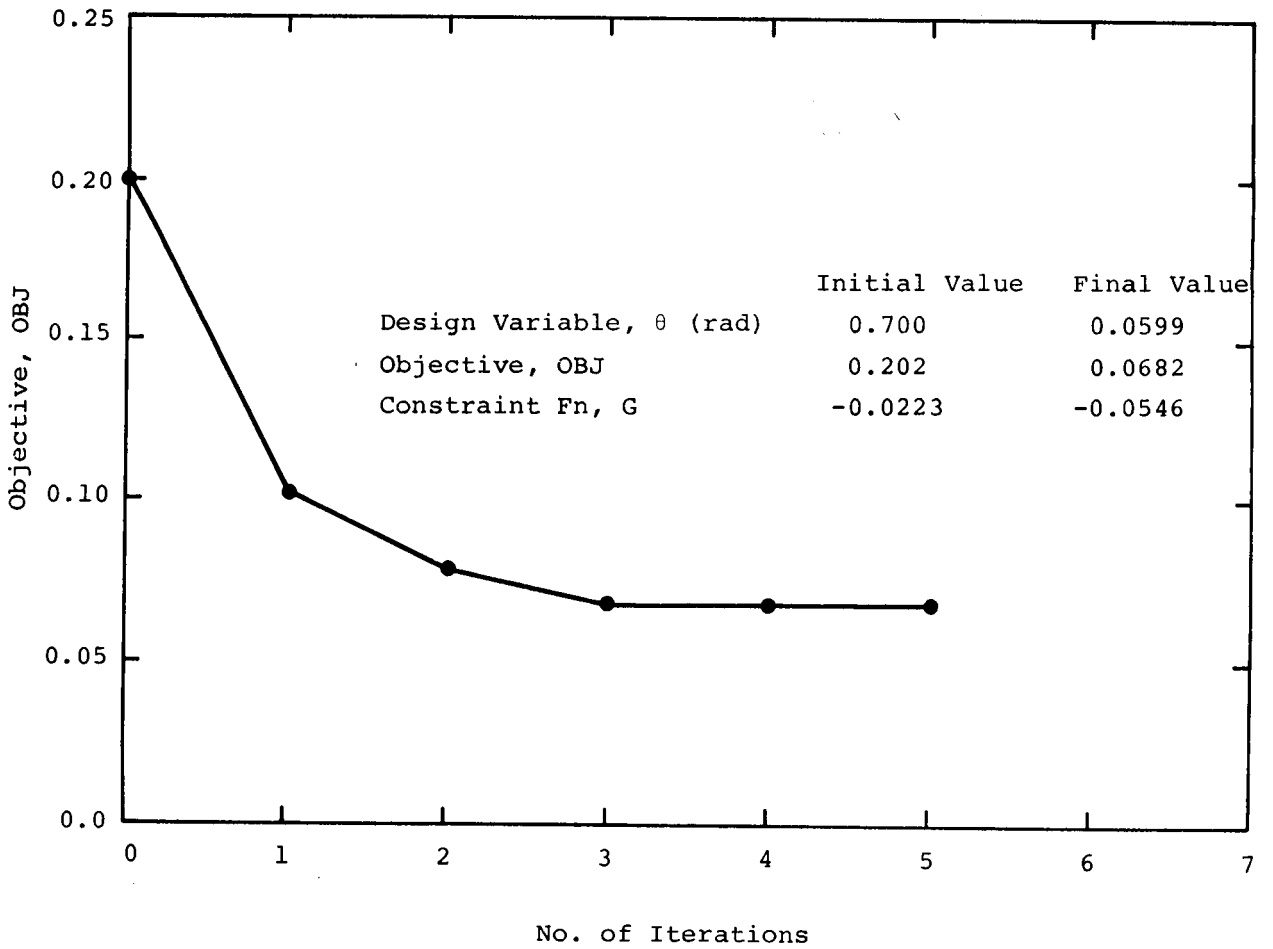

Figure 7

OPTIMIZATION EXAMPLE 2

An iteration history for the second optimization example is shown in figure 8. Here θ_1 and θ_2 were unlinked, and the flutter constraint was removed. The initial values of θ_1 and θ_2 were 0 deg and 45 deg, respectively. Convergence was achieved in five iterations with $\theta_1 = 0.334$ deg and $\theta_2 = 1.53$ deg. This is clearly the valley near the origin in design space suggested by figure 5.

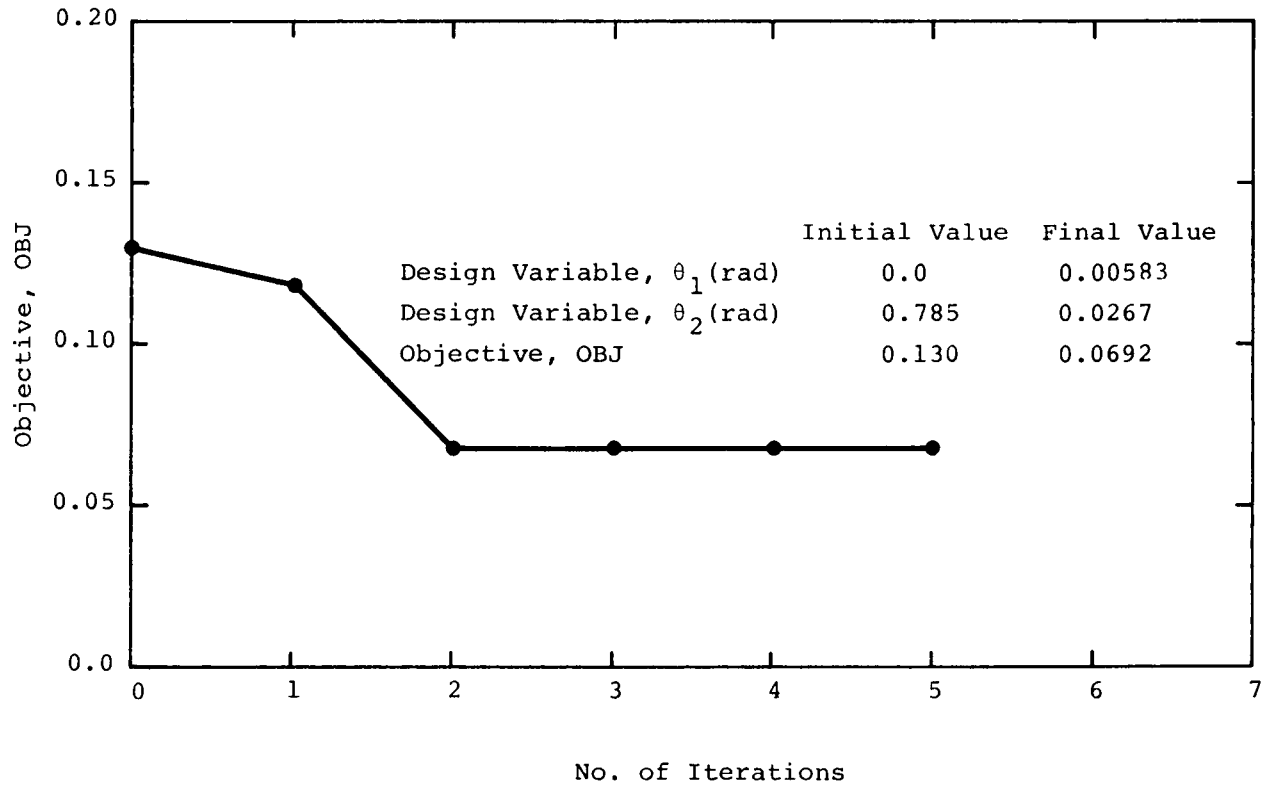

Figure 8

OPTIMIZATION EXAMPLE 3

The third optimization example is an attempt to find a neighboring valley in the design space. The starting point was at $\theta_1 = 10$ deg, $\theta_2 = 70$ deg, with no constraints other than side constraints on the design variables. The iteration history for this example is shown in figure 9. The minimum found here is at $\theta_1 = 2.20$ deg, $\theta_2 = 92.5$ deg, a neighboring valley with a minimum not quite as low as that near the origin.

Ironically, the best design -- the one with the most forward location of the center of pressure -- is the one initially chosen, with the "zero-deg" plies in the spanwise direction. From the standpoint of tailoring, this example is clearly not a very attractive one, since the movement of the center of pressure is not substantial. Different layups, and particularly those with more bending-twist coupling, would produce more appealing results.

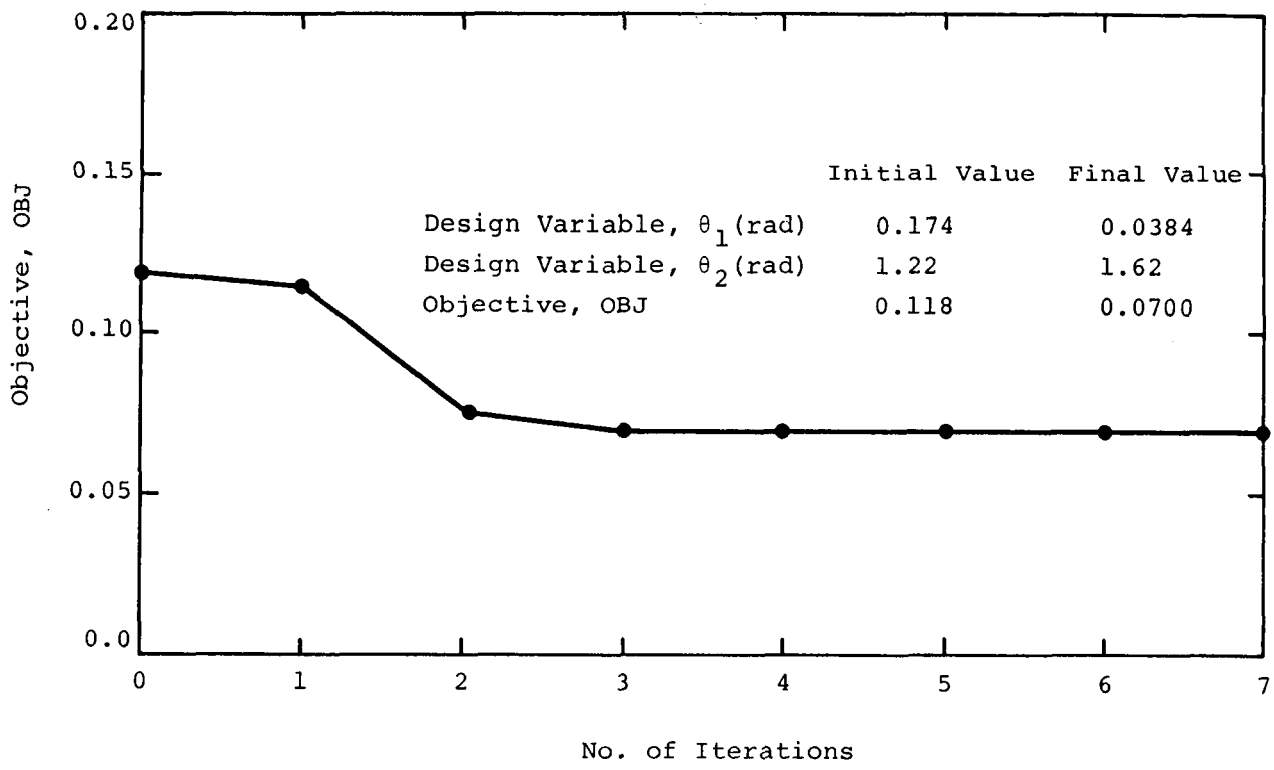

Figure 9

REFERENCES

1. Dillenius, M. F. E. and McIntosh, S. C., Jr.: Aeroelastic Procedure for Controlling Hinge Moments. AIAA Paper 88-0528, presented at the AIAA 26th Aerospace Sciences Meeting (Reno, Nevada), January 1988.

2. Przemieniecki, J. S.: Theory of Matrix Structural Analysis. McGraw Hill, New York, 1968.

3. Zienkiewicz, O. C.: The Finite Element Method. McGraw-Hill (UK), London, 1977.

4. Dillenius, M. F. E.: Program LRCDM2, Improved Aerodynamics Prediction Program for Supersonic Canard-Tail Missiles with Axisymmetric Bodies. NASA CR-3883, April 1985.

5. Vanderplaats, G. N.: CONMIN - A Fortran Program for Constrained Function Minimization. User's Manual. NASA TM X-62,282, August 1973. Addendum, May 1978.

ACKNOWLEDGEMENTS

The work described in this paper was performed as a Phase I Small Business Innovation Research (SBIR) project sponsored under NAVAIR Contract N00019-86-C-0032 and is being continued as a Phase II SBIR project under NAVAIR Contract N00019-88-C-0071.